Supplementary Information for

From Waste to Precious: Recovering and Anchoring Au from Electronic Wastewater onto Poly m-Phenylenediamine Membrane for Catalytic Nitrophenol Conversion

Youmei Xu[§a], Yuchao Chen[§a], Mengxia Wang[a, b], Yufei Shu[a], Siyu Cao[a], Zhongying Wang[a, c], *

[a] School of Environmental Science and Engineering, Southern University of Science and Technology, Shenzhen 518055, China

[b] School of Environment, Harbin Institute of Technology, Harbin 150001, China

[c] Guangdong Provincial Key Laboratory of Soil and Groundwater Pollution Control, Southern University of Science and Technology, Shenzhen 518055, China

§ The authors contributed equally to the work.

* To whom correspondence should be addressed. E-mail: wangzy6@sustech.edu.cn
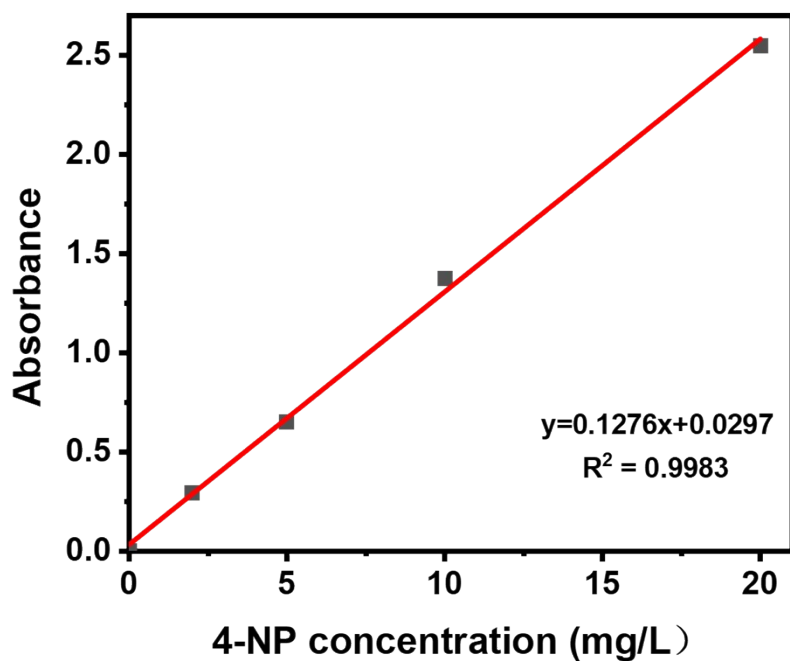
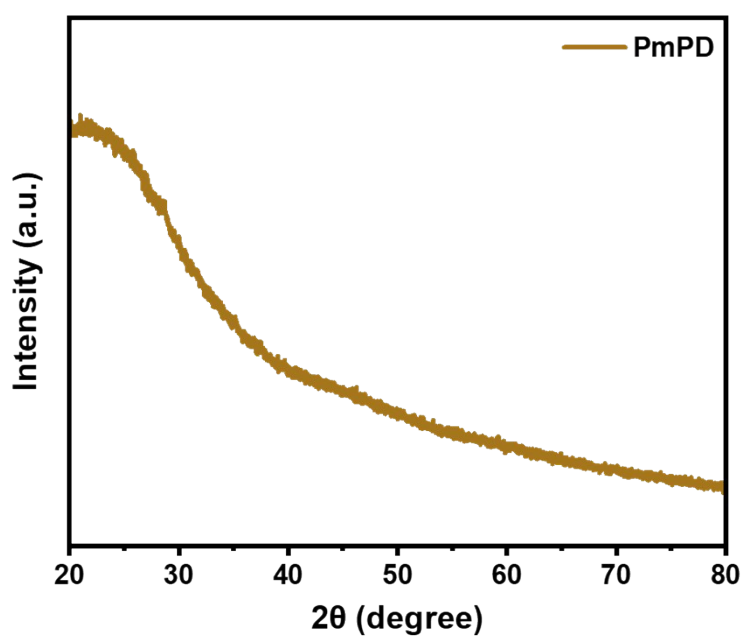FIGURE S1 Concentration-absorbance standard curve of 4-NP.

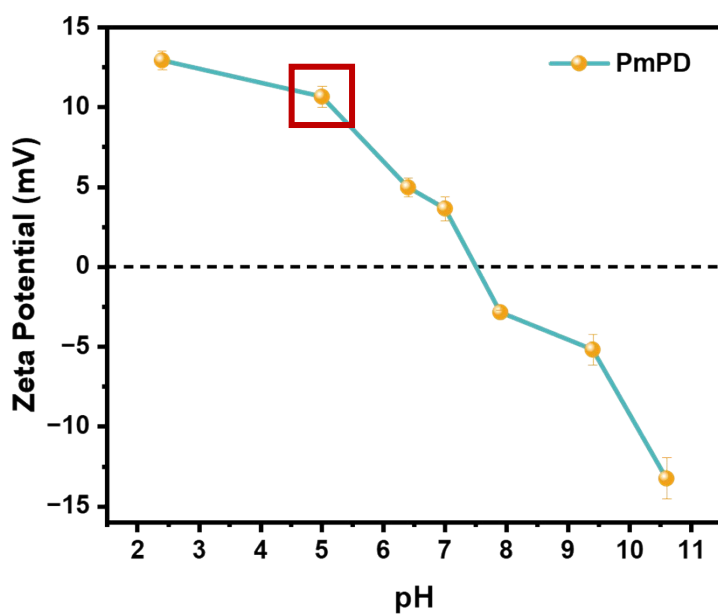FIGURE S2 XRD pattern of PmPD nanoparticles.

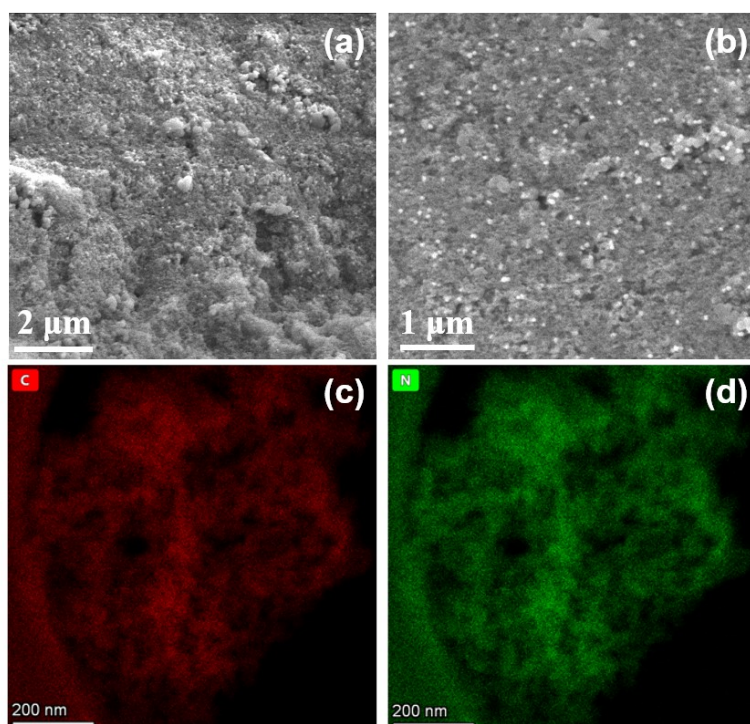FIGURE S3 Plot of zeta potential versus pH for cross-linked PmPD.

FIGURE S4 (a, b) SEM images, (c) C, (d) N elemental mapping of Au@PmPD membrane.
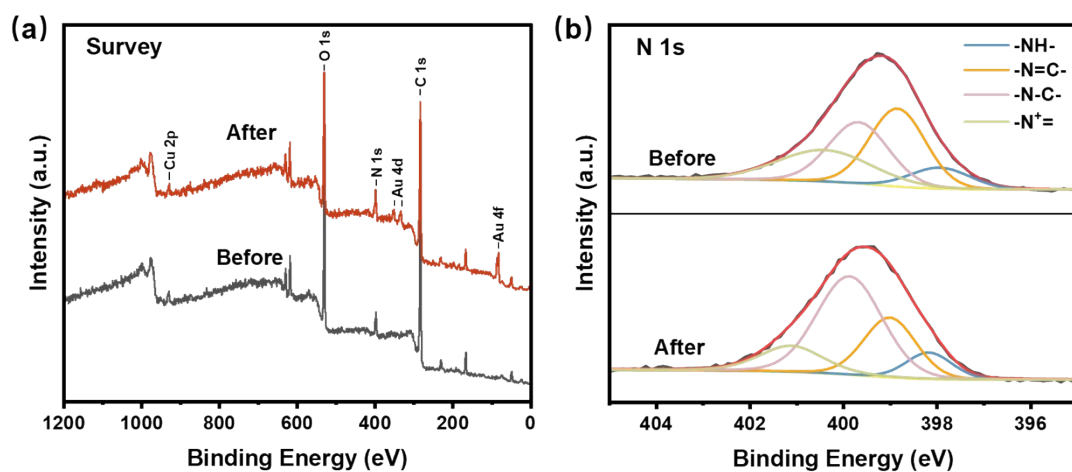
FIGURE S5 The (a) survey and (b) high-resolution N 1s XPS spectra of PmPD membrane before and after Au(III) recovery.
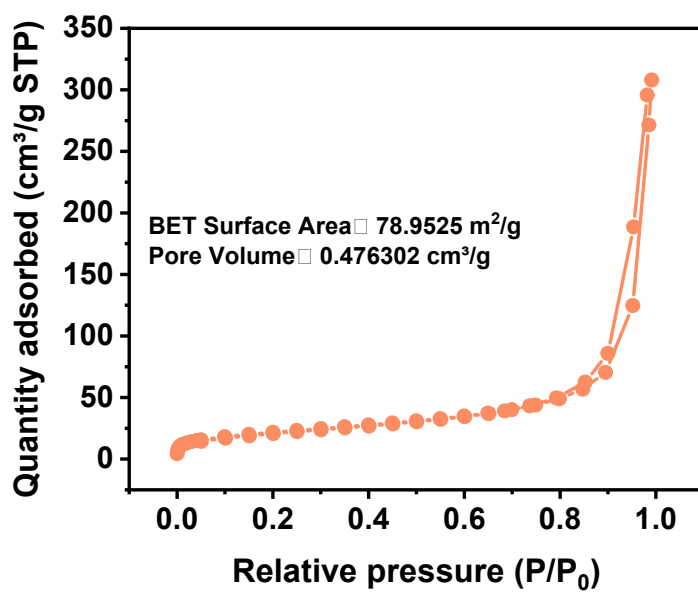

FIGURE S6 N$_2$ adsorption-desorption isotherm of Au@PmPD.

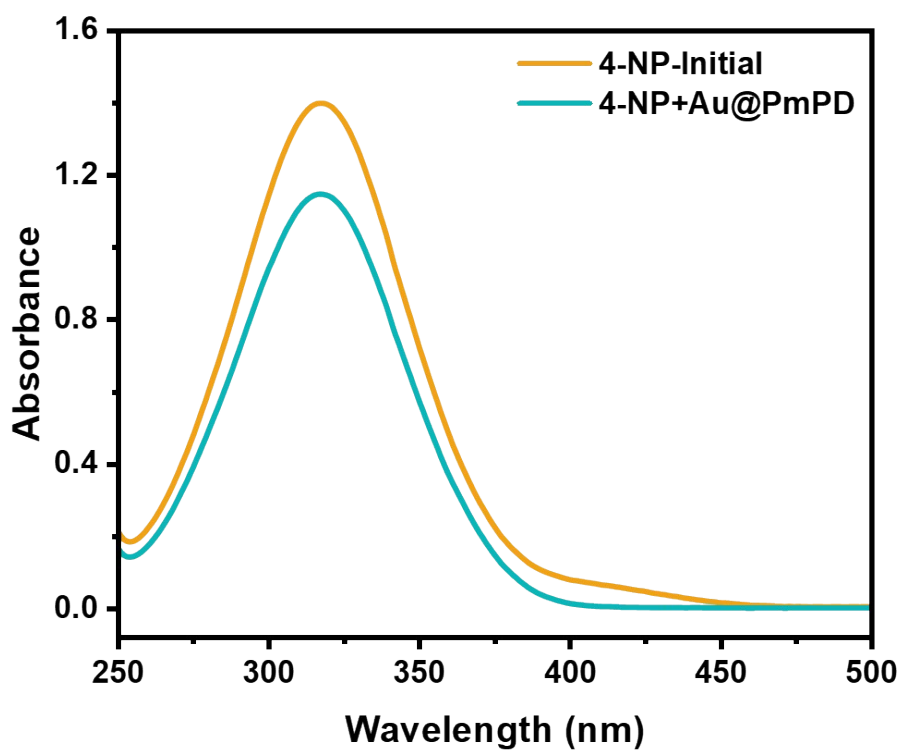FIGURE S7 UV-vis absorbance changes of 4-NP before and after passing through Au@PmPD membrane.
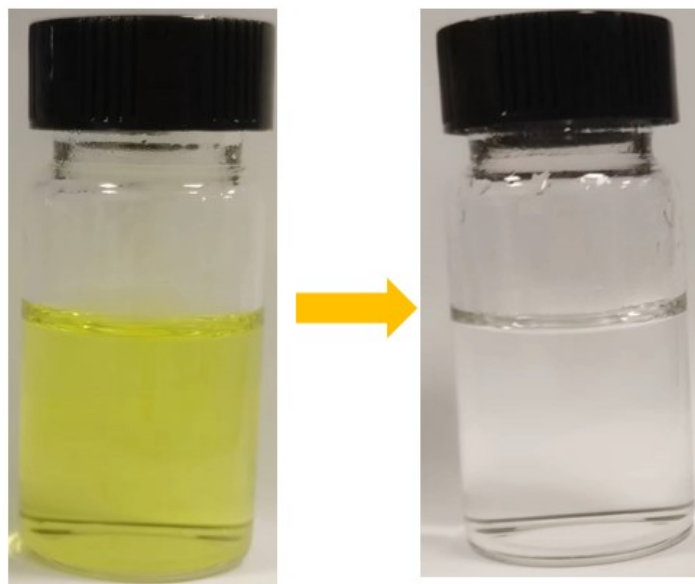
FIGURE S8 Color change of 4-NP solution before and after catalytic reduction reaction through the Au@PmPD membrane.
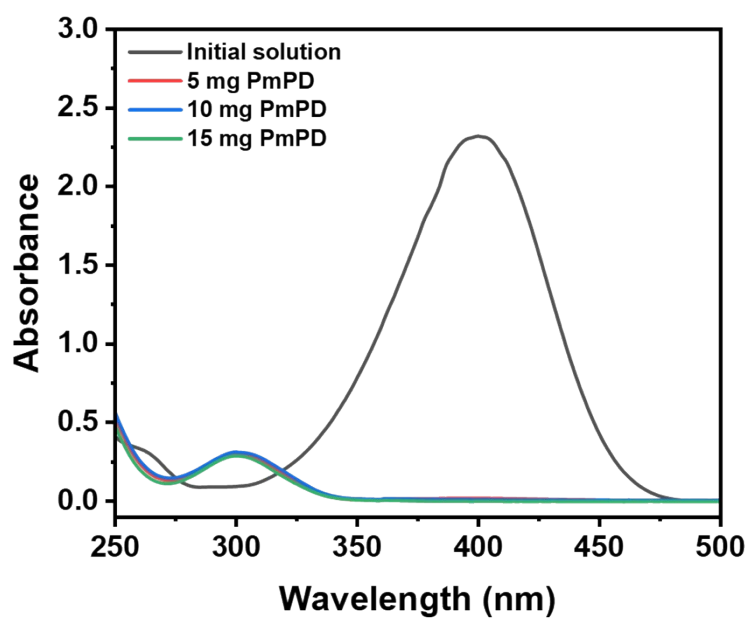
FIGURE S9 The effect of PmPD loading on the catalytic performance of Au@PmPD membrane.
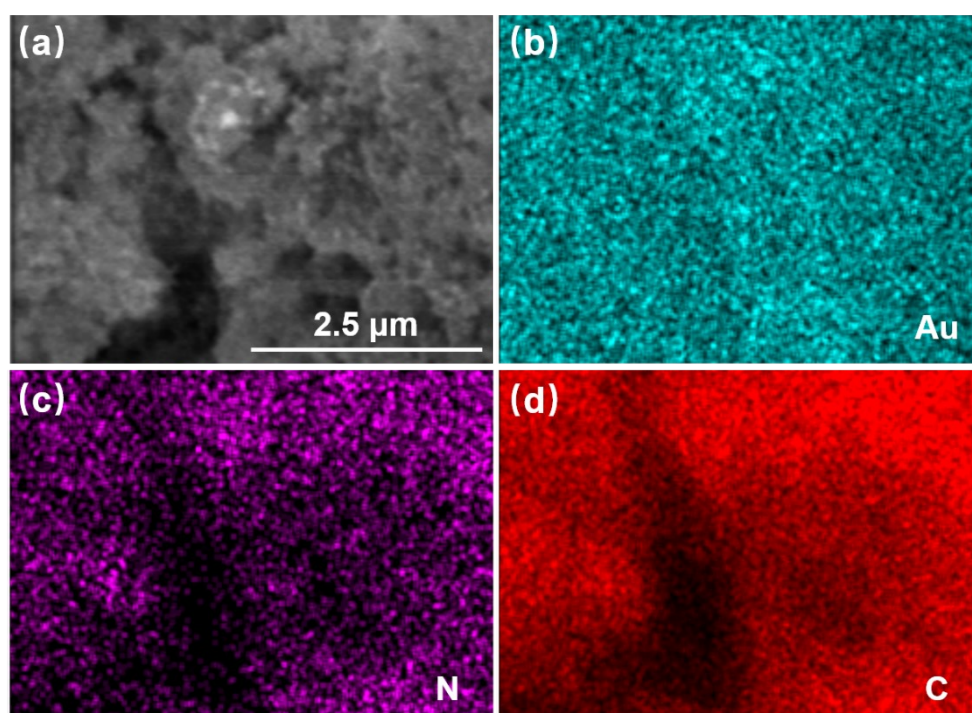
FIGURE S10 (a) SEM image, (b) Au, (c) N, (d) C elemental mapping spectra of the Au@PmPD membrane after 136-min reaction.

FIGURE S11 Plot of flux and residence time versus pressure for the Au@PmPD membrane.
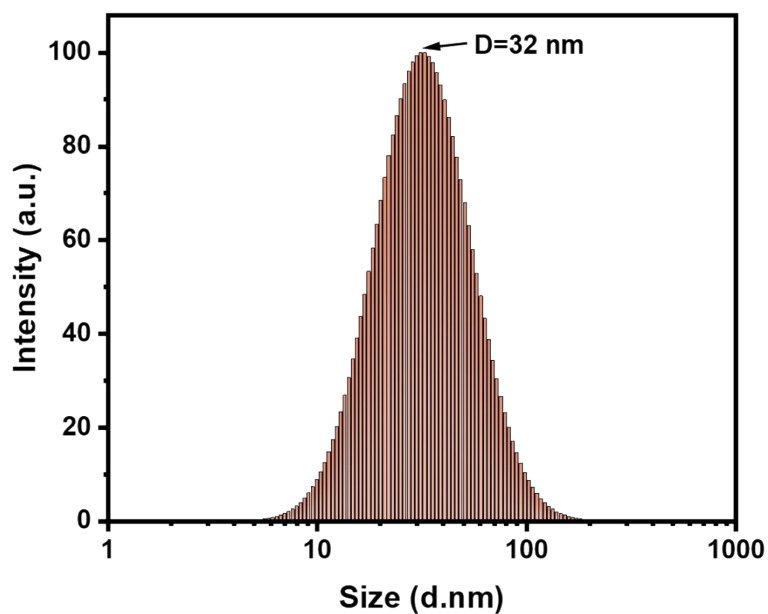
FIGURE S12 Size distribution of Au NPs dispersion.
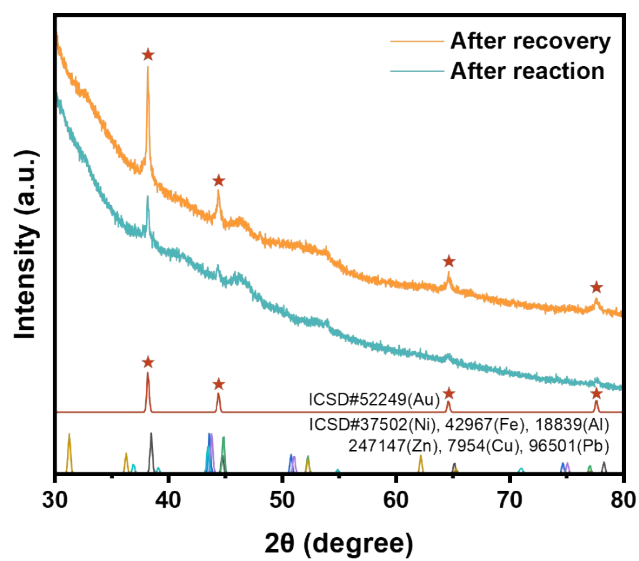
FIGURE S13 XRD patterns of the PmPD membranes after electronic wastewater recovery and the following catalytic reaction.

Text S1 The measurement of effective pore volume (V_{eff}).

To determine the effective pore volume of the Au@PmPD membrane, a "water-filling" method was employed.[1, 2] The experimental procedure involved the following specific steps: Firstly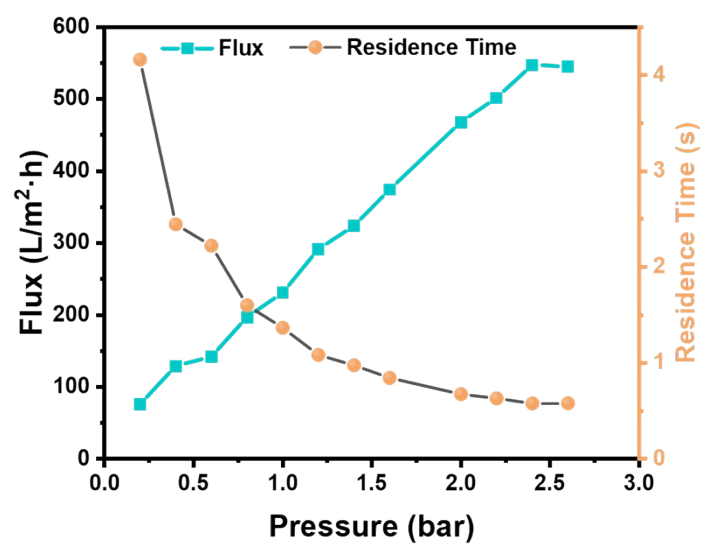, the mass of the dry nylon membrane substrate was denoted as m_0. Subsequently, the membrane was immersed in water and weighed as m_1. Then the masses of Au@PmPD membrane containing 15 mg PmPD and 4.0 mg Au NPs in dry (m_2) and wet states (m_3) were measured. Finally, the amount of water present in the membrane pores was utilized to calculate the effective pore volume (V_{eff}, cm^3) of the Au@PmPD membrane, employing Equation S1:

$$V_{eff} = \frac{(m_3 - m_2) - (m_1 - m_0)}{\rho_{H_2O}} \qquad \text{S1}$$

Table S1 Comparison of catalytic reduction of 4-NP by Au@PmPD membrane with the membranes reported in published literature.

Membrane Catalyst	4-NP (mM)	NaBH$_4$ (mM)	K value (s^{-1})	conversion	References
Nanoporous Cu/Cu$_2$O	0.067	34	0.024	>95%	[3]
PET-DOPA-PEI-GNP	0.2	20	0.0041	>99%	[4]
Cu-Ag-Au NPs@β-LGF	0.29	300	0.038	~89%	[5]
Pd0 NPs@SPES-C	0.5	50	0.0132	~90%	[6]
AgNPs/ESM	0.29	300	0.0042	>95%	[7]
AuNCs/CNTs	0.15	28.13	0.033	>99%	[8]
HCNM-AuNPs	0.2	50	0.0133	>99%	[9]
Ag/TiO$_2$/PVDF@TiO$_2$	0.1	10	1.47	>96%	[10]
Au@PmPD	0.14	25	2.206	>99%	This work

Table S2 Characteristics of simulated electronic wastewater.

pH		-0.92
c/(mg·L^{-1})	Cu^{2+}	15700
	Fe^{3+}	4440.5
	Zn^{2+}	2010
	Al^{3+}	1985
	Ni^{2+}	675.5
	Pb^{2+}	19.54
	Au^{3+}	5.55

Table S3 Quality characteristics of simulated dyeing wastewater.

	methylene blue (MB)	100
$c/(\text{mg}\cdot\text{L}^{-1})$	4-nitrophenol (4-NP)	20
	NaCl	1000
pH		10.2
Conductivity/$(\mu\text{S}\cdot\text{cm}^{-1})$		2074

References:

1. Zhang, S.; Sun, M.; Hedtke, T.; Deshmukh, A.; Zhou, X.; Weon, S.; Elimelech, M.; Kim, J. Mechanism of Heterogeneous Fenton Reaction Kinetics Enhancement under Nanoscale Spatial Confinement. *Environ. Sci. Technol.* **2020**, *54*(17), 10868-10875.

2. Zhang, S.; Hedtke, T.; Zhu, Q.; Sun, M.; Weon, S.; Zhao, Y.; Stavitski, E.; Elimelech, M.; Kim, J. Membrane-Confined Iron Oxychloride Nanocatalysts for Highly Efficient Heterogeneous Fenton Water Treatment. *Environ. Sci. Technol.* **2021**, *55*(13), 9266-9275.

3. Bai, X.; Chen, D.; Li, Y.; Yang, X.; Zhang, M.; Wang, T.; Zhang, X.; Zhang, L.; Fu, Y.; Qi, X.; Qi, W. Two-dimensional MOF-derived nanoporous Cu/Cu2O networks as catalytic membrane reactor for the continuous reduction of p-nitrophenol. *J. Membrane Sci.* **2019**, *582*, 30-36.

4. Subair, R.; Tripathi, B.P.; Formanek, P.; Simon, F.; Uhlmann, P.; Stamm, M. Polydopamine modified membranes with in situ synthesized gold nanoparticles for catalytic and environmental applications. *Chem. Eng. J.* **2016**, *295*, 358-369.

5. Huang, R.; Zhu, H.; Su, R.; Qi, W.; He, Z. Catalytic Membrane Reactor Immobilized with Alloy Nanoparticle-Loaded Protein Fibrils for Continuous Reduction of 4-Nitrophenol. *Environ. Sci. Technol.* **2016**, *50*(20), 11263-11273.

6. Domènech, B.; Muñoz, M.; Muraviev, D.N.; Macanás, J. Catalytic membranes with palladium nanoparticles: From tailored polymer to catalytic applications. *Catal. Today.* **2012**, *193*(1), 158-164.

7. Liang, M.; Su, R.; Qi, W.; Yu, Y.; Wang, L.; He, Z. Synthesis of well-dispersed Ag nanoparticles on eggshell membrane for catalytic reduction of 4-nitrophenol. *J. Mater. Sci.* **2014**, *49*(4), 1639-1647.

8. Liu, Y.; Zheng, Y.; Du, B.; Nasaruddin, R.R.; Chen, T.; Xie, J. Golden Carbon Nanotube Membrane for Continuous Flow Catalysis. *Ind. Eng. Chem. Res.* **2017**, *56*(11), 2999-3007.

9. Wang, H.; Dong, Z.; Na, C. Hierarchical Carbon Nanotube Membrane-Supported Gold Nanoparticles for Rapid Catalytic Reduction of p-Nitrophenol. *ACS Sustain. Chem. Eng.* **2013**, *1*(7), 746-752.

10. Wang, Y.; Ma, S.; Huang, M.; Yang, H.; Xu, Z.; Xu, Z. Ag NPs coated PVDF@TiO2 nanofiber membrane prepared by epitaxial growth on TiO2 inter-layer for 4-NP reduction application. *Sep. Purif. Technol.* **2019**, *227*, 115700.